



Structure of a Longitudinal Actin Dimer Assembled by Tandem W Domains: Implications for Actin Filament Nucleation

Grzegorz Rebowksi¹†, Suk Namgoong¹†, Malgorzata Boczkowska¹, Paul C. Leavis², Jorge Navaza³ and Roberto Dominguez^{1*}

¹Department of Physiology, University of Pennsylvania School of Medicine, 3700 Hamilton Walk, Philadelphia, PA 19104-6085, USA

²Boston Biomedical Research Institute, Watertown, MA 02472-2899, USA

³Institut de Biologie Structurale, F-38027 Grenoble, France

Received 27 May 2010;
received in revised form
30 July 2010;
accepted 20 August 2010
Available online
8 September 2010

Edited by R. Craig

Keywords:

actin nucleation;
W domain;
nucleation-promoting factors;
Tβ4;
actin monomer sequestration

Actin filament nucleators initiate polymerization in cells in a regulated manner. A common architecture among these molecules consists of tandem WASP homology 2 domains (W domains) that recruit three to four actin subunits to form a polymerization nucleus. We describe a low-resolution crystal structure of an actin dimer assembled by tandem W domains, where the first W domain is cross-linked to Cys374 of the actin subunit bound to it, whereas the last W domain is followed by the C-terminal pointed end-capping helix of thymosin β4. While the arrangement of actin subunits in the dimer resembles that of a long-pitch helix of the actin filament, important differences are observed. These differences result from steric hindrance of the W domain with intersubunit contacts in the actin filament. We also determined the structure of the first W domain of *Vibrio parahaemolyticus* VopL cross-linked to actin Cys374 and show it to be nearly identical with non-cross-linked W-Actin structures. This result validates the use of cross-linking as a tool for the study of actin nucleation complexes, whose natural tendency to polymerize interferes with most structural methods. Combined with a biochemical analysis of nucleation, the structures may explain why nucleators based on tandem W domains with short inter-W linkers have relatively weak activity, cannot stay bound to filaments after nucleation, and are unlikely to influence filament elongation. The findings may also explain why nucleation-promoting factors of the Arp2/3 complex, which are related to tandem-W-domain nucleators, are ejected from branch junctions after nucleation. We finally show that the simple addition of the C-terminal pointed end-capping helix of thymosin β4 to tandem W domains can change their activity from actin filament nucleation to monomer sequestration.

© 2010 Elsevier Ltd. All rights reserved.

*Corresponding author. E-mail address:

droberto@mail.med.upenn.edu.

† G.R. and S.N. contributed equally to this work.

Abbreviations used: W domain, WASP homology 2 domain; Tβ4, thymosin β4; NPF, nucleation-promoting factor; SAXS, small-angle X-ray scattering; PDB, Protein Data Bank; D-loop, DNase I binding loop.

Introduction

Nucleation of actin filaments in cells is kinetically unfavorable because of the instability of polymerization intermediates (dimers, trimers, and tetramers) and the actions of actin monomer binding proteins

such as profilin and thymosin β 4 (T β 4).^{1,2} This creates an opportunity for cells to use molecules known as actin filament nucleators to initiate the formation of actin polymerization nuclei in a spatially and temporally controlled manner.

The actin filament can be described as either a single left-handed short-pitch helix, where consecutive subunits are staggered with respect to one another by half a monomer length, or two right-handed long-pitch helices of head-to-tail bound actin subunits.^{3–5} Different nucleators work via different mechanisms, stabilizing small actin oligomers along either the long-pitch helices or the short-pitch helix of the actin filament.^{6,7}

Most actin filament nucleators use the WASP homology 2 domain (W domain) for interaction with actin. The W domain has a short length (17–27 amino acids) and is extremely abundant and functionally versatile.^{7–9} The N-terminal portion of the W domain forms a helix that binds in the hydrophobic (or target binding) cleft¹⁰ formed between subdomain 1 and subdomain 3 at the barbed end of the actin monomer.^{11–13} After this helix, the W domain presents an extended region that is directed towards the pointed end of the actin monomer (formed by subdomains 2 and 4 of actin). This region is variable in length and sequence but comprises the conserved four-residue motif LKKT(V), which is critical for the interaction with actin.¹¹

Filament nucleators are characterized by the presence of multiple actin-binding sites. The simplest and most common architecture consists of tandem repeats of the W domain, occurring in the proteins Spire,¹⁴ Cobl,¹⁵ and VopL/VopF.^{16,17} The W domain also participates in filament nucleation through nucleation-promoting factors (NPFs) of the Arp2/3 complex, which can have between one W domain and three W domains.^{18–20} The muscle-specific nucleator Lmod also contains one W domain.²¹ The nucleation activities of nucleators based on tandem W domain vary widely. The reason for these differences may lie, at least in part, in the highly variable linkers between W domains. When the linkers are short, as in the relatively weak nucleator Spire,¹⁴ only actin subunits along the long-pitch helix of the actin filament can be connected. In contrast, the brain-enriched protein Cobl is a strong nucleator (featuring three W domains with a long linker between its second W domain and its third W domain) and is thought to stabilize a short-pitch actin trimer for nucleation.¹⁵ Examples of Cobl, the Arp2/3 complex, and formins suggest that stabilization of a short-pitch actin nucleus is a more effective way to promote polymerization than stabilization of a long-pitch actin nucleus.^{6,7} However, the structural bases for this observation are not well understood.

In an attempt to understand the nucleation mechanism of nucleators based on tandem W

domain, we recently reported a solution study, using small-angle X-ray scattering (SAXS), of an actin dimer and a trimer stabilized by tandem-W-domain constructs.²² These complexes, referred to as 2W-Actin and 3W-Actin and containing two and three W domains, respectively, were capped at the barbed end by structure-based cross-linking of the first W domain to Cys374 of the first actin subunit and at the pointed end by addition of the C-terminal helix of T β 4. Constructs 2W and 3W are based on the W-domain repeat present in the NPF protein N-WASP (*neuronal Wiskott–Aldrich syndrome protein*), which, like Spire, presents short inter-W linkers. The SAXS study suggested that the actin subunits in the complexes adopted an elongated conformation similar to that of the long-pitch helix of the actin filament. However, the resolution of this study was insufficient to establish a direct comparison between the longitudinal contacts of actin subunits in the complexes and the longitudinal contacts of actin subunits in the actin filament.

Here we report the crystal structure of 3W-Actin at 7 Å resolution. Only two actin subunits are present in the structure, indicating that one of the actin subunits is released during crystallization. Despite its low resolution, this structure, obtained by fitting high-resolution structures of W-Actin complexes into the low-resolution data, offers a clearer picture of the relative disposition of actin subunits bound to tandem W domains that are separated by Spire-like short inter-W linkers. While the longitudinal arrangement of actin subunits in the structure is somewhat related to that of the long-pitch helix of the actin filament,^{3,4} important differences are observed. These differences probably result from steric hindrance of the W domain with intersubunit contacts in the filament. Determination of the 3W-Actin structure was aided by the determination of the 2.9-Å-resolution crystal structure of the first W domains of VopL¹⁶ cross-linked to actin Cys374 (referred to as WxActin). The structure of WxActin is nearly indistinguishable from non-cross-linked W-Actin structures determined previously,^{11–13} thus validating the use of cross-linking as a tool to stabilize actin polymerization complexes for structural investigation. The structures, as well as a biochemical analysis of nucleation, reveal important clues about existing disparities in the nucleation activities of nucleators based on tandem W domain.

Results and Discussion

Crystal structure of cross-linked WxActin

In two previous studies, we reported low-resolution SAXS structures of actin nucleation complexes formed by the Arp2/3 complex and tandem W

domains.^{22,23} Barbed-end polymerization in these studies was blocked by cross-linking of the W domain to Cys374 of the actin subunit located at the barbed end of the complexes. This approach was based on an analysis of the structures of various W-Actin complexes,^{11–13} which placed the N-terminus of the W domain within disulfide bond distance of actin Cys374. In each case, a Cys residue was introduced into the W domain at the most favorable position for cross-linking to actin Cys374. Here, this approach was used again to obtain the low-resolution crystal structure of 3W-Actin. However, it remained unclear whether the cross-link altered the structure of actin and/or the W domain in a significant way, prompting us to pursue the determination of a

crosslinked WxActin structure. It later became apparent that this structure also provided the best molecular replacement model for the determination of the 3W-Actin structure.

After testing crystallization with various W domains, we obtained good-diffracting crystals of the cross-linked complex of actin with a synthetic peptide corresponding to the first W domain (amino acids 130–160) of *Vibrio parahaemolyticus* VopL. During synthesis, residue Val131 of this W domain was replaced by Cys and cross-linked to actin Cys374 (Materials and Methods). The crystal structure of WxActin was determined by molecular replacement up to 2.9 Å resolution (Fig. 1a and Table 1).

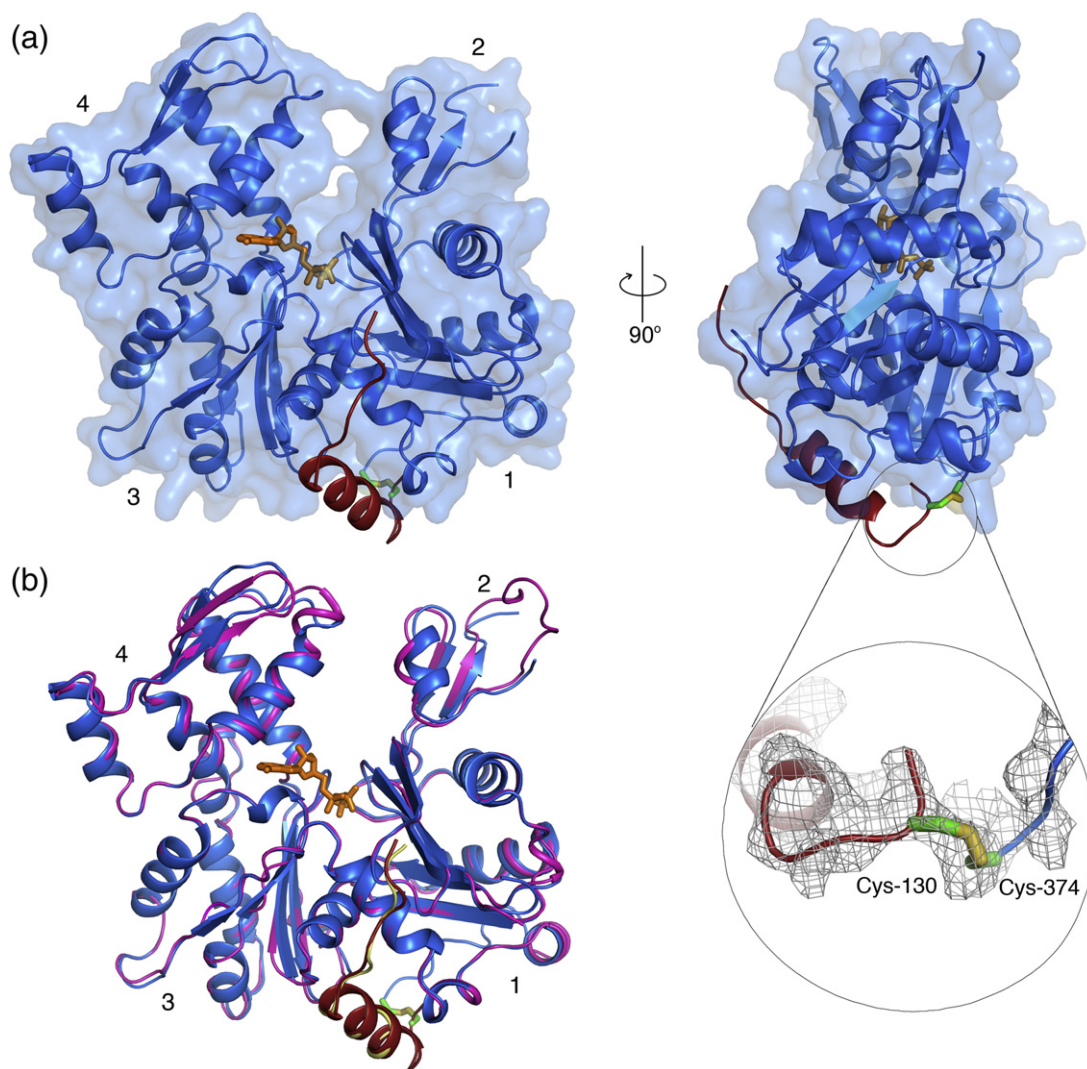


Fig. 1. Structure of WxActin. (a) Two perpendicular views of the structure of WxActin. Inset: The $2F_o - F_c$ electron density map (contoured at 1σ) in the region around the cross-link. Although the cross-link was visualized, this is one of the less well-defined regions of the map. (b) Superimposition of the structures of WxActin (blue, actin; red, W domain) and the non-cross-linked complex of actin with the W domain of WASP (pink, actin; yellow, W domain) showing the similarity of the structures.

Table 1. Crystallographic data and refinement statistics

| | WxActin | 3W-Actin |
|--|--------------------------|------------------------------------|
| <i>Diffraction data</i> | | |
| Wavelength (Å) | 1.0 | 1.0 |
| Space group | $P2_12_12_1$ | $P6_522$ |
| Unit cell parameters <i>a</i> , <i>b</i> , <i>c</i> (Å) | 66.6, 76.4, 86.1 | 100.7, 100.7, 458.8 |
| Unit cell parameters α , β , γ (°) | 90.0, 90.0, 90.0 | 90.0, 90.0, 120.0 |
| Resolution (Å) | 50.0–2.89 (2.99–2.89) | 50.0–7.0 (7.9–7.0) |
| Unique reflections | 10,207 | 2182 |
| Completeness (%) | 99.2 (92.5) | 90.0 (70.1) |
| Redundancy | 12.9 (6.4) | 20.5 (6.0) |
| R_{merge}^a (%) | 16.8 (46.1) | 8.6 (37.3) |
| I/σ | 16.3 (1.8) | 16.5 (2.1) |
| <i>Refinement</i> | | |
| Resolution (Å) | 37.51–2.89 | |
| Atoms used in refinement | 3058 | |
| R -factor ^b (%) | 21.2 | |
| R_{free}^c (%) | 26.5 | No atomic refinement was performed |
| rmsd bond lengths (Å) | 0.011 | |
| rmsd bond angles (°) | 1.910 | |
| Average <i>B</i> -factors (Å ²) | | |
| All atoms | 62.90 | |
| Protein atoms | 62.92 | |
| Solvent | 58.57 | |
| Residues in Ramachandran plot | | |
| Most favored regions (%) | 90.2 | |
| Other allowed regions (%) | 9.8 | |
| PDB accession code | 3M1F | 3M3N |
| Values in parentheses correspond to the highest-resolution shell. | | |
| ^a $R_{\text{merge}} = \sum_{hkl} (I - \langle I \rangle) / \sum I$, where <i>I</i> and $\langle I \rangle$ are the observed and mean intensities, respectively, of all the observations of reflection <i>hkl</i> , including its symmetry-related equivalents. | | |
| ^b $R\text{-factor} = \sum_{hkl} F_{\text{obs}} - F_{\text{calc}} / \sum F_{\text{obs}} $, where F_{obs} and F_{calc} are the observed and calculated structure factors of reflection <i>hkl</i> , respectively. | | |
| ^c R_{free} and R -factor were calculated for a randomly selected subset of reflections (5%) that were not used in refinement. | | |

The structure of WxActin is very similar to those of non-cross-linked W-Actin complexes determined with bound DNase I^{11,13} and that of *Drosophila* ciboulot bound to actin-latrunculin A.¹² Figure 1b shows a comparison of the structure of WxActin with that of the non-cross-linked complex of actin with the W domain of WASP [Protein Data Bank (PDB) accession code 2A3Z]. The two structures superimpose with an rmsd of 0.66 Å for 358 equivalent C α atoms. The most important differences occur in regions that were visualized in one of the structures, but not in the other, including the DNase I binding loop (D-loop), the C-terminus of actin, and the N-terminus of the W domain. The D-loop is disordered in most structures of actin, as well as in the structure of WxActin described here, but forms an extended β -sheet with β -strands of DNase I in the non-cross-linked structure. The C-terminus of actin is also disordered in most

crystal structures, except in complexes with profilin, which interacts with the C-terminus of actin.^{24–26} In the non-cross-linked W-Actin complex, the last 10 amino acids of actin (Gly366-Phe375) are disordered, and the W domain is only visualized starting from WASP residue Arg431 (corresponding to VopL Asn132). In contrast, in the cross-linked structure, only the last amino acid of actin (Phe375) is unresolved in the electron density map, whereas the W domain of VopL is visualized from residue 130 to residue 151 (i.e., the last nine amino acids of the synthetic peptide were not resolved). The disulfide bond between actin Cys374 and VopL Cys131 is visualized in the electron density map (Fig. 1a, inset), although it is poorly defined compared to the rest of the structure.

The similarity of the structures suggests that the cross-linking approach used here and in previous studies^{22,23} as a tool to cap the barbed end of actin polymerization nuclei for structural investigation does not introduce significant structural distortions. Furthermore, as we show next, the availability of the WxActin structure aided the determination of the 3W-Actin structure.

Crystal structure of 3W-Actin

The solution SAXS study of 3W-Actin revealed an elongated molecule—consistent with the presence of three actin subunits—that seemed somewhat similar to the long-pitch helix of the actin filament.²² However, the nature of actin–actin contacts in the complex could not be determined. We suggested that subdomain 2 of actin could move slightly; this, combined with a helical conformation in the D-loop, would make the binding of tandem W domains fully compatible with intersubunit contacts in the actin filament.^{3,4} Other investigators suggested that the W domain would probably interfere with intersubunit contacts in the filament.^{27,28} Knowing which proposal is correct is important because it may shed light on the mechanism of nucleation and may possibly explain why nucleators based on tandem W domain do not influence elongation the way formins do. It may also answer important questions about differences in the activities of nucleators based on tandem W domain and in the mechanisms of action of the NPFs of the Arp2/3 complex, which also contain tandem W domains.⁷ Therefore, we set out to crystallize the complexes of 2W-Actin and 3W-Actin. While both complexes were crystallized readily, the crystals did not diffract the X-rays. Additional search for conditions led to the identification of additives, such as RbCl and polyvinylpyrrolidone K15, that somewhat improved diffraction. After several attempts, the best result consisted of a rather complete and highly redundant X-ray data set collected from crystals of 3W-Actin up to 7 Å resolution. While we initially considered not

reporting this structure, we later recognized that significant information could be obtained by positioning high-resolution W-Actin structures into the unit cell of 3W-Actin crystals by molecular replacement. Because the individual structures are known at high resolution, this approach overcomes some of the typical limitations of low-resolution structures in which the content of the unit cell is totally unknown. The limitations, however, are that individual atomic positions cannot be refined and inter-W linkers cannot be visualized.

Consistent with its design and the mass measurements in solution of the 3W-Actin complex,²² three copies of the W-Actin basic unit were expected in the asymmetric unit of the crystal. The volume of the asymmetric unit was also compatible with the presence of three copies of the W-Actin unit, which would have resulted in a solvent content of 43%. However, weak diffraction is typically consistent with a higher solvent content. Not surprisingly, the molecular replacement solution, performed independently with the programs PHENIX^{29,30} and AMoRe,³¹ located only two W-Actin complexes in the asymmetric unit for a solvent content of 62% (see [Materials and Methods](#) and a detailed description in Supplementary Material). We do not understand why one of the actin molecules dissociates during crystallization, although it could simply be that this molecule is bound loosely and is therefore displaced by favorable crystal contacts. Analysis of crystal packing demonstrates why a third actin molecule was never found. Consecutive actin dimers are stacked head-to-tail, forming a helix along the crystallographic *c* axis (Movie S1). Two such helices assemble tightly in anti-parallel fashion (see Movie S2). Each anti-parallel pair comprises 24 actin subunits along the length of the *c* axis, which constitutes the basic building block of the crystal lattice. Adjacent pairs of helices cross over twice in a repeat (or helical turn), corresponding to the length of the *c* axis (see Movies S3 and S4), thus ensuring the connectivity of the crystal lattice and leaving no extra space for the missing third actin subunit (or rather 12 actin subunits when the P6₅22 symmetry of the crystal is taken into consideration).

Because of the limited resolution, we could not identify which of the actin subunits is lost during crystallization, or whether the crystals consist solely of the actin subunit cross-linked to the long 3W polypeptide. Note that any non-cross-linked actin dissociated from the complex would be expected to polymerize during crystallization and would therefore not be present in the crystals. To address this question, we collected a large number of crystals, washed them multiple times in the crystallization solution by transferring them with a cryo loop, and then dissolved them in water for analysis by nonreducing gel electrophoresis and mass spectrometry ([Materials and Methods](#)). The results

clearly illustrate that the crystals consist of a 50/50 mixture of actin cross-linked to construct 3W and non-cross-linked actin (Fig. 2a). Therefore, we conclude that one of the non-cross-linked actins was lost during crystallization, which, based on the arrangement of actin subunits in the asymmetric unit, is most likely that bound to the last W domain.

The disposition of actin subunits in the structure of 3W-Actin (Fig. 2b) is somewhat similar to the longitudinal arrangement of actin subunits in the long-pitch helix of the actin filament model^{3,4} (Fig. 2c). However, important differences are observed. For a better understanding of these differences, it is important to discuss what is currently known about longitudinal contacts in the actin filament. Multiple crystal structures of actin show similar longitudinal contacts between actin subunits (including both noncrystallographic dimers and symmetry-related dimers), which are thought to mimic intersubunit contacts in the actin filament (Table 2). However, because of constraints imposed by crystal symmetry, these dimers are unwound (i.e., they lack the natural twist of the actin filament). A detailed analysis of these structures and their implications for our understanding of the actin filament has been carried out by other investigators³⁷ and will not be repeated here. However, it is important to compare the structure of 3W-Actin to the actin filament model^{3,4} and the longitudinal dimers observed in crystal structures, with the understanding that the structure of 3W-Actin does not address the conformation of the actin filament *per se* but rather the mechanism of recruitment of actin subunits by tandem-W-domain proteins.

The dimers observed in crystal structures are generally similar and often crystallographically isomorphous. Based on a superimposition of their structures, we have identified three subgroups that diverge more significantly (represented by PDB accession codes 2FXU, 1Y64, and 2HMP) (Table 2). Compared to a long-pitch dimer of the actin filament model in which consecutive subunits are rotated by $\sim 27^\circ$,^{3,4} these three subgroups present flat structures [i.e., rotated counterclockwise with respect to the filament dimer by approximately -27° (Fig. 2d), although the orientation of the axis of rotation is markedly different for entry 2HMP]. Remarkably, longitudinal contacts between subdomain 4 and subdomain 3 of neighboring actin subunits are well conserved in the three subgroups (Fig. 3). It thus appears that longitudinal contacts between actin subunits in the filament have a strong tendency to reemerge as crystal contacts in actin structures.³⁷ It is important to note that these structures offer the most accurate view of longitudinal contacts currently available³⁷ because the resolution of the actin filament model^{3,4} is still insufficient to address specific atomic interactions. Additional longitudinal contacts are thought to involve the D-loop in sub-

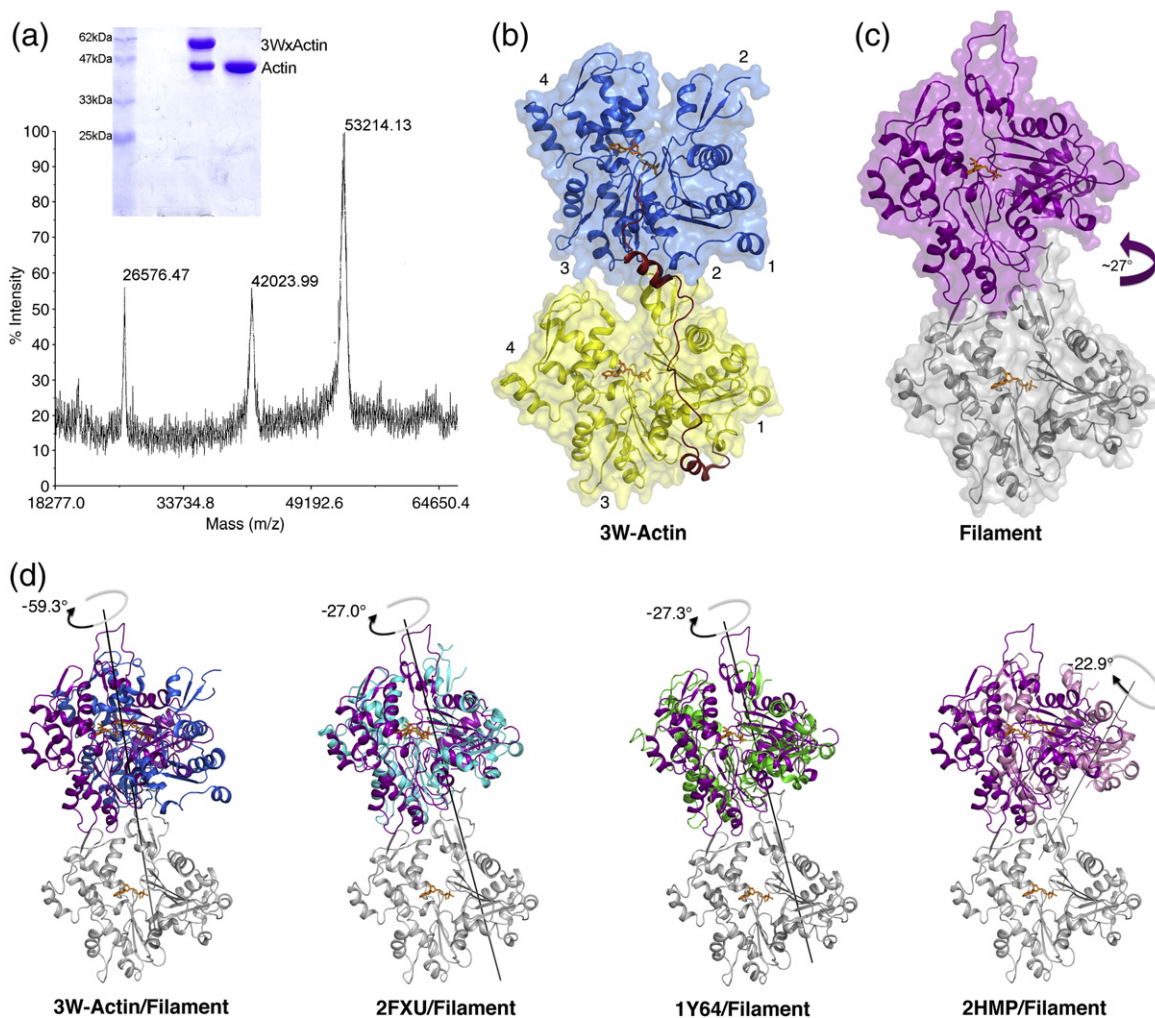


Fig. 2. Structure of 3W-Actin. (a) Nonreducing gel electrophoresis and mass spectrometry analysis indicate that the crystals of 3W-Actin consist of a 50/50 mixture of actin cross-linked to construct 3W (expected mass, 53,021 Da) and non-cross-linked actin. Actin is also shown in the gel as control. (b) Illustration of the structure of 3W-Actin. The linker between W domains was modeled. (c) Illustration of a longitudinal actin dimer from the actin filament model.⁴ (d) Comparisons of the relative rotations between actin subunits in the actin filament model (gray and magenta) and the structures of 3W-Actin and three representative actin dimers observed in crystal structures (including noncrystallographic and symmetry-related dimers; see also Table 2). For this comparison, the structures were superimposed using as reference the lower actin subunit (gray), which is only shown for the filament model. Note that, compared to a long-pitch dimer of the actin filament in which subunits are rotated by $\sim 27^\circ$ (magenta arrow), there is a -60° rotation between the two crystallographically independent actin subunits in the structure of 3W-Actin. Other dimers observed in crystal structures tend to be flat due to symmetry constraints and are therefore rotated -27° relative to a longitudinal dimer of the filament. The relative rotations between actin subunits were calculated with the program DynDom.³²

domain 2,⁴⁰ which is proposed to bind in the hydrophobic cleft between subdomain 1 and subdomain 3 of the actin subunit immediately above it.⁴ However, the D-loop is disordered in all crystal structures containing longitudinal actin dimers, and its conformation(s) and actual contacts in the filament are unknown.

On the other hand, the rotation between the two actin subunits in the structure of 3W-Actin is approximately -33° (i.e., -60° compared with a longitudinal dimer of the actin filament)^{3,4} (Fig. 2d).

As a result, the longitudinal contacts observed in other crystal dimers are generally broken in the structure of 3W-Actin (Fig. 3), whereas the contacts involving subdomain 2 are unresolved. Therefore, it appears that the presence of the W domain at the interface between actin subunits breaks the natural tendency of actin to preserve filament-like longitudinal contacts in crystal structures and induces a rotation between actin subunits that is of similar magnitude to, but in the opposite direction of, the filament (-33° versus 27°). These results are generally

Table 2. Structures of longitudinal actin dimers

| PDB accession code | Actins per asymmetric unit | Description | Symmetry | Resolution (Å) | Cell parameters | | References |
|----------------------|----------------------------|---|--------------|----------------|--|---------------------------------------|---|
| | | | | | <i>a</i> , <i>b</i> , <i>c</i> (Å) | α , β , γ (°) | |
| 3M3N | 2 | Dimer stabilized by tandem W domains | $P6_522$ | 7.0 | 100.7, 100.7, 458.8 | 90.0, 90.0, 120.0 | This work |
| 2HF3 2HF4 | 1 | Nonpolymerizable actin mutant (Ala204Glu/Pro243Lys) | $C2$ | 1.8 | 199.7, 54.1, 39.6 | 90.0, 93.2, 90.0 | Rould <i>et al.</i> ³³ |
| 2ASM 2ASO 2ASP | 1 | Complexes with marine macrolides | $C2$ | 1.6 or 1.35 | 171.2, 54.7, 40.7 or 60.1, 56.5, 101.7 | 90.0, 96.0, 90.00 or 90.0, 94.6, 90.0 | Allingham <i>et al.</i> ³⁴ and Rizvi <i>et al.</i> ³⁵ |
| 2FXU 2A5X | 1 | Longitudinally cross-linked actin dimer | $C2$ | 2.49 | 207.4, 54.4, 36.2 | 90.0, 98.6, 90.0 | Kudryashov <i>et al.</i> ³⁶ |
| 2Q1N 2Q31 | 2 | Longitudinally cross-linked actin dimer | $P2_1$ | 2.7 | 108.1, 71.8, 54.8 | 90.0, 104.7, 90.0 | Sawaya <i>et al.</i> ³⁷ |
| 1Y64 | 1 | Complex with formin homology 2 domain | $C2$ | 3.05 | 232.0, 56.2, 100.9 | 90.0, 107.7, 90.0 | Otomo <i>et al.</i> ³⁸ |
| 2HMP | 2 | Nonpolymerizable actin, cleaved between Gly42 and Val43 | $P2_12_12_1$ | 1.9 | 64, 198, 69.6 | 90.0, 90.0, 90.0 | Klenchin <i>et al.</i> ³⁹ |

consistent with our previous SAXS studies,²² which revealed an extended (pseudo-long-pitch) arrangement of the actin subunits stabilized by tandem W domains. However, the SAXS envelope lacked the resolution to distinguish between the dimer observed here in the crystal structure of 3W-Actin and a longitudinal dimer of the actin filament model.

It is interesting to note that there is also a crystal contact in the structure of 3W-Actin (between two adjacent dimers) that resembles the dimer of the asymmetric unit. This so-called ‘crystal’ dimer differs even more significantly from both the actin filament and the other actin dimers described above due to an overall translation of ~ 8 Å between actin

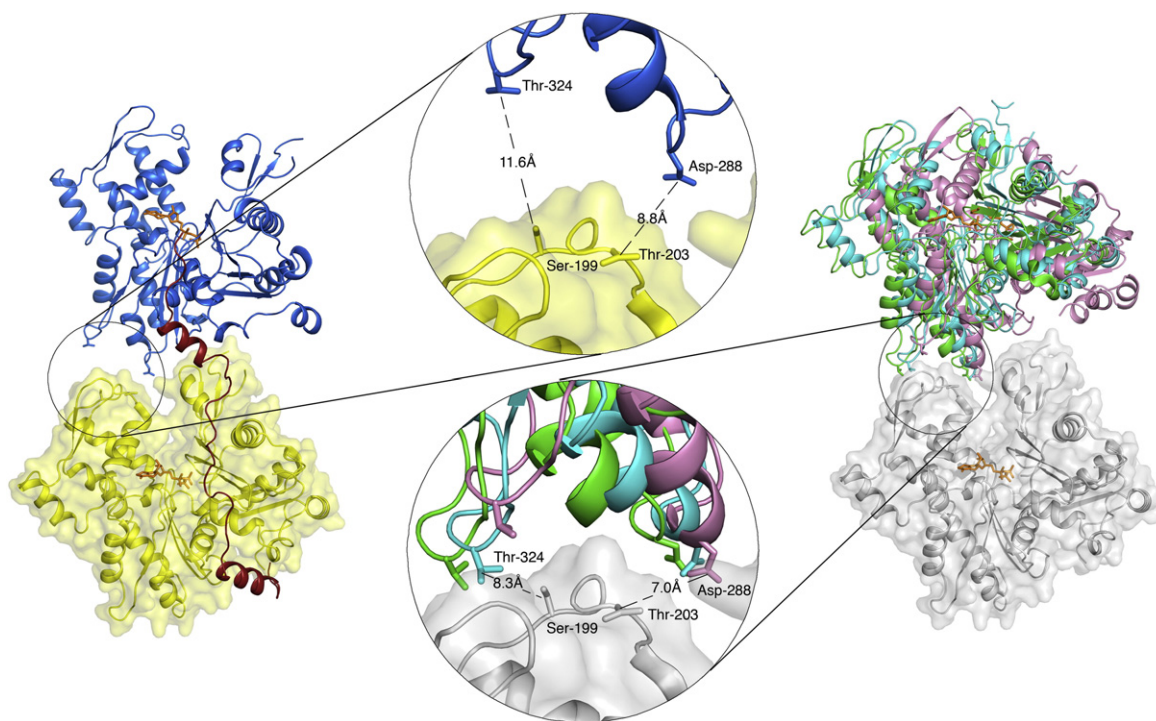


Fig. 3. Intersubunit contacts in the structure of 3W-Actin compared to those in the structures of crystallographic actin dimers. Insets: Longitudinal contacts between subdomain 4 and subdomain 3 of adjacent actin subunits observed in various crystal structures (right) are mostly broken in the structure of 3W-Actin (left). Representative distances between C^{β} atoms are shown for reference.

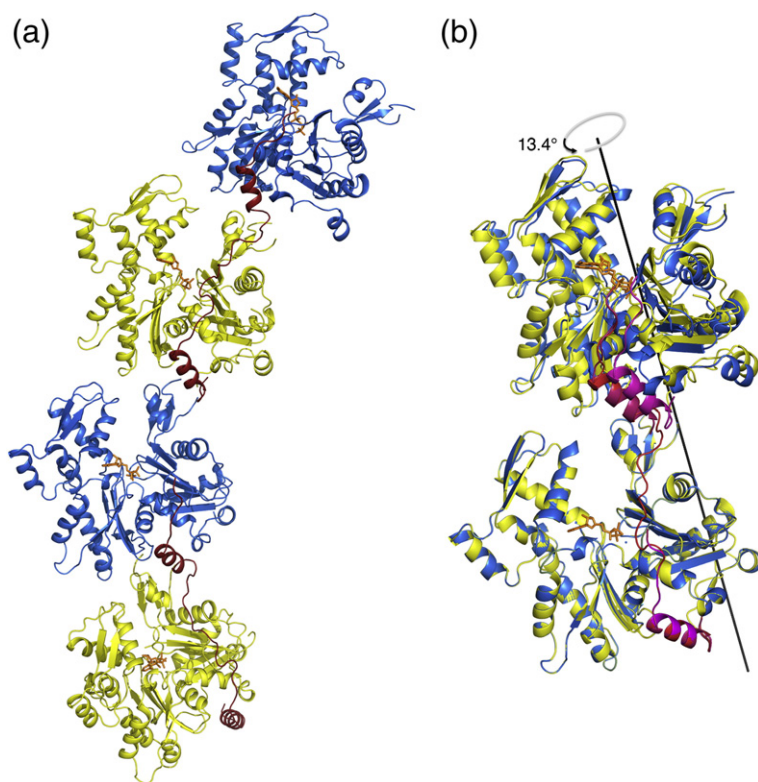


Fig. 4. Comparison of noncrystallographic and crystallographic dimers in the structure of 3W-Actin. (a) Representation of two consecutive dimers related by crystal symmetry. (b) Superimposition of noncrystallographic (yellow-blue and red W domains) and crystallographic (blue-yellow and magenta W domains) dimers. Note that, despite their general similarity, the crystallographic dimer differs more significantly from other actin dimers observed in crystals structures (Table 2) and the actin filament model. While the actin subunits in the crystallographic dimer are rotated $\sim 13^\circ$ relative to the noncrystallographic dimer, which undoes part of the initial -60° rotation, there is also a translation of $\sim 8 \text{ \AA}$, probably imposed by steric hindrance with the cross-linked W domain. It is nonetheless significant that the actin subunits of both noncrystallographic and crystallographic dimers are rotated counterclockwise by about the same amount compared to all the other dimers observed in

crystal structures, which are generally unwound (see Fig. 2), suggesting that this is a general property of the W domain at the interface between actin subunits.

subunits compared to the dimer of the asymmetric unit (Fig. 4). In the crystal dimer, the cross-link with construct 3W is at the interface between actin subunits, which may explain the added translation. However, it is significant that the actin subunits of both noncrystallographic and crystal dimers are rotated counterclockwise by about the same amount compared to all the other actin dimers observed in crystal structures, suggesting that this is a general constraint imposed by the W domain at the interface between actin subunits.

We conclude that while Spire-like tandem W domains can bring actin subunits into close proximity for nucleation, the conformation of the polymerization nucleus formed differs significantly from that of the actin filament. This may explain their weak nucleation activity, as analyzed next.

Long-pitch nucleation by tandem W domains is suboptimal

The structural results prompted us to test the polymerization activity of construct 3W as compared to that of the prototypical tandem-W-domain nucleator Spire, which stabilizes a long-pitch nucleus, and that of the Arp2/3 complex, which forms a short-pitch nucleus. The nucleation activity of *Drosophila* Spire¹⁴ has been mapped to the fragment Spire_{366–482} comprising the four W domains (Fig. 5a),

which was used in the current study. We used the pyrene-actin polymerization assay to study the effect of Spire_{366–482} on the polymerization of $2 \mu\text{M}$ actin (6% pyrene labeled) by monitoring the fluorescence increase resulting from the incorporation of labeled actin monomers into the filament (Fig. 5b). At a concentration of 25 nM, Spire_{366–482} had very little effect on actin polymerization (polymerization rate of $1.0 \pm 0.2 \text{ nM/s}$ versus $0.8 \pm 0.1 \text{ nM/s}$ for actin alone), whereas the Arp2/3 complex activated by the WCA fragment of mouse N-WASP showed a major increase in polymerization (polymerization rate, $31.5 \pm 1 \text{ nM/s}$). However, the nucleation activity of Spire_{366–482} increased with concentration, becoming a stronger nucleator at 250 nM (polymerization rate, $4.8 \pm 0.2 \text{ nM/s}$). The opposite effect was observed with construct 3W, which had no effect on actin polymerization at a concentration of 25 nM but inhibited polymerization when used at 250 nM. This could be an indication that construct 3W, like T β 4, sequesters actin monomers (Fig. 5b).

T β 4 is a short 43-amino-acid polypeptide related to the W domain^{8,9} but contains an additional helix at the C-terminus that binds atop actin subdomains 2 and 4⁴¹ (Fig. 5a). As a result and despite the apparent simplicity of its helix-loop-helix design, T β 4 has the ability to block actin monomer addition to both the pointed end and the barbed end of the actin filament, making it an extremely effective

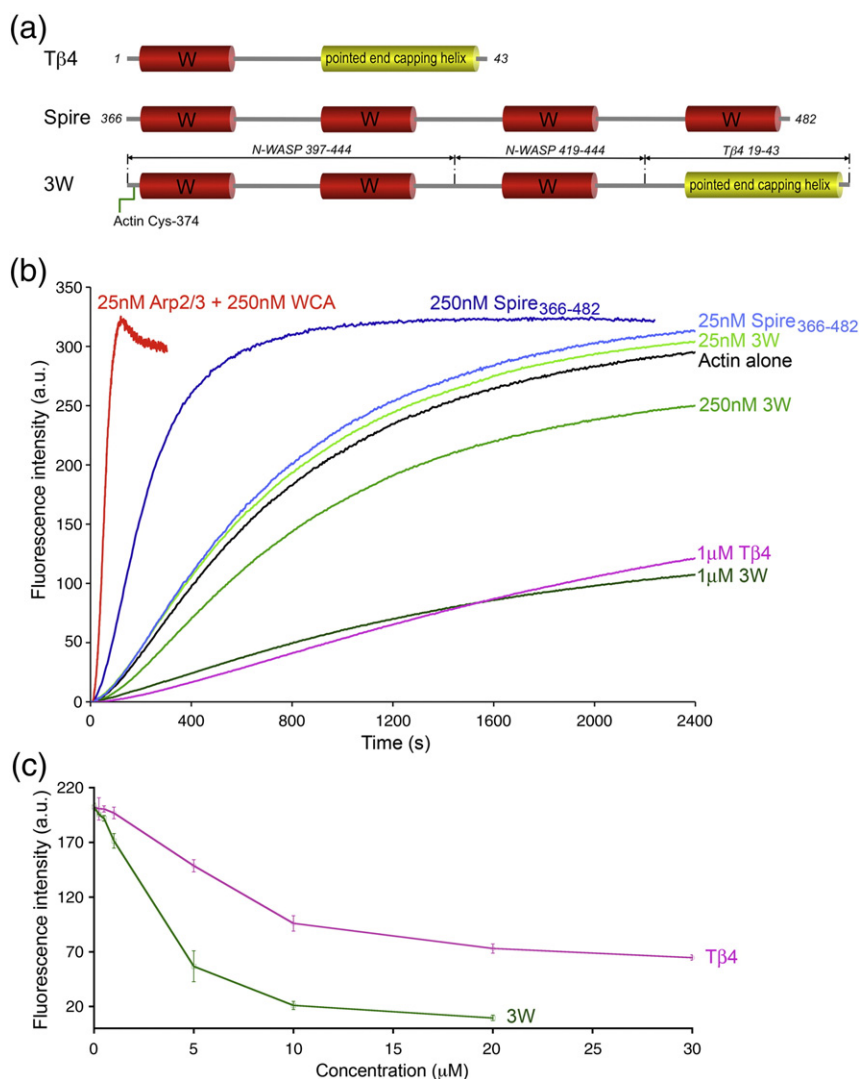


Fig. 5. 5 Different effects of Spire, 3W, and T β 4 on actin polymerization. (a) Schematic diagram of T β 4, the four W-domain region of *Drosophila* Spire, and construct 3W. Note that construct 3W consists of three W domains (occurring naturally in mouse N-WASP) separated by short linkers (as in Spire) and the pointed end-capping helix of T β 4. This construct also contains a Cys residue at the N-terminus that was cross-linked to actin Cys374 for crystallization, but the cross-link was reduced with DTT to measure nucleation activity. (b) Time course of polymerization of 2 μ M Mg-ATP-actin (6% pyrene labeled) alone (black) or in the presence of different concentrations of Spire₃₆₆₋₄₈₂ (different shades of blue), construct 3W (different shades of green), T β 4 (pink), and 25 nM Arp2/3 complex with 250 nM WCA fragment of mouse N-WASP (red). Each experiment was repeated at least three times. The polymerization rates are as follows: actin (0.8 ± 0.1 nM/s), Spire (1.0 ± 0.2 nM/s at 25 nM; 4.8 ± 0.2 nM/s at 250 nM), Arp2/3 complex (31.5 ± 1 nM/s). (c) Steady-state concentration dependence of actin monomer sequestration by T β 4 and 3W.

monomer-sequestering protein.^{42,43} Some proteins contain tandem repeats of the T β 4 fold. Examples include *Acanthamoeba castellanii* actobindin,⁴⁴ *Drosophila melanogaster* ciboulot,¹² and *Caenorhabditis elegans* tetrathymosin,⁴⁵ which contain 2.5, 3, and 4 copies of the T β 4 fold, respectively. Contrary to tandem repeats of the W domain, which frequently mediate filament nucleation,⁷ tandem T β 4 proteins are characterized by their ability to sequester actin monomers.^{44,45} Therefore, we asked whether 3W, consisting of a tandem repeat of three W domains

followed by the C-terminal helix of T β 4 (Fig. 5a), would sequester actin monomers. A concentration dependence analysis of steady-state actin polymerization revealed that construct 3W sequesters actin monomers even more effectively than T β 4 (Fig. 5c). We have previously shown, using analytical ultracentrifugation, light scattering, and native gel electrophoresis, that 3W binds three actin monomers in solution,²² which may explain its stronger sequestering activity compared to T β 4. Therefore, the effect of 3W on actin polymerization is more

closely related to that of tetrathymosin, which binds and sequesters multiple actin monomers.⁴⁵ Although actobindin and ciboulot also sequester actin monomers, perhaps surprisingly they form 1:1 complexes with actin, indicating that only one of their actin-binding sites is fully functional.^{12,44} It thus appears that the simple addition of the pointed end-capping helix of T β 4 to tandem W domains changes their activity from nucleation, as in Spire,¹⁴ to monomer sequestration, as in T β 4.^{42,43}

Conclusions

The crystal structure of cross-linked WxActin was found to be nearly indistinguishable from those of non-cross-linked W-Actin complexes. We have used W-domain cross-linking in this work, as well as in two previous studies.^{22,23} The finding that the structure is not altered in a significant way by the cross-link suggests that this is a structurally sound approach that can be used as a way to stabilize large polymerization complexes, which are intrinsically dynamic, for structural investigation.

Various proteins contain tandem repeats of the W domain.^{7–9} While the W domain itself presents well-conserved features (N-terminal helix and LKKT(V) motif), the linkers between W domains are highly variable, and no single structure can be fully representative of this large family of proteins. Irrespective of this variability, inter-W linkers can be subdivided into two subgroups: short (as in Spire and N-WASP) and long (as in Cobl linker 2). While 3W is a synthetic construct with no natural counterpart, it is based on the tandem W repeat of N-WASP and therefore represents the short inter-W linker subgroup. One general implication of the structure of its complex with actin is that the binding of the W domain is intrinsically incompatible with intersubunit contacts along the long-pitch helix of the actin filament, contrary to what we had anticipated.^{3,4} The structure of 3W-Actin further suggests that the actin subunits recruited by tandem W domains with short inter-W linkers are positioned in a way that resembles the long-pitch helix of the actin filament—a conformation that would be expected to favor polymerization. However, due to steric hindrance of the W domain, the contacts between actin subunits in these complexes differ significantly from those of the actin filament. This may explain the weak nucleation activity of Spire as compared to the nucleation activities of the Arp2/3 complex, formins, Cobl, and Lmod—proteins that are thought to stabilize short-pitch actin nuclei to initiate polymerization. The incompatibility of the W domain with longitudinal intersubunit contacts in the filament also implies that when the actin nucleus transitions into a filament and begins to elongate, tandem-W-domain nucleators cannot stay bound to

newly formed filaments and would therefore be unlikely to influence elongation. Steric hindrance of the W domain may also be a contributing factor in the release of the NPFs of the Arp2/3 complex from branch junctions once the branch filament begins to elongate (conformational changes within the Arp2/3 complex itself could be another factor). We finally found that the simple addition of the C-terminal pointed end-capping helix of T β 4 to tandem W domains can change their activity from actin filament nucleation to monomer sequestration.

Materials and Methods

Preparation of proteins and protein complexes

A detailed description of the preparation and characterization of the 3W-Actin complex,²² as well as of the purification of the Arp2/3 complex from bovine brain and the preparation of the WCA fragment of mouse N-WASP,²³ was reported previously. Actin was purified from rabbit skeletal muscle.⁴⁶ T β 4 and the first W domain (amino acids Ser130–Ser160) of *V. parahaemolyticus* VopL (UniProt accession code Q87GE5) were made as synthetic peptides and purified by reverse-phase chromatography. During peptide synthesis, an amino acid substitution (Val131 → Cys) was made in the first W domain of VopL (a position chosen based on an analysis of the various W-Actin structures)^{11–13} as it is most favorable for cross-linking to actin Cys374. The cross-linking reaction was performed by activation of the W-domain peptide with 5,5'-dithiobis(2-nitrobenzoic acid) before its mixture with actin at an actin/W peptide ratio of 1:1.2. The cross-linked fraction was then separated by gel filtration on an S200 column (Pfizer-Pharmacia) in 25 mM Tris–HCl (pH 7.5), 100 mM NaCl, 0.2 mM CaCl₂, and 0.2 mM ATP.

Fragment 366–482 of *Drosophila* Spire (Spire_{366–482}), comprising the four W domains, was amplified by PCR from cDNA (Open Biosystems). The PCR product was cloned between the NdeI site and the EcoRI site of vector pTYB12 (New England BioLabs). Protein expression was performed in BL21(DE3) cells (Invitrogen) grown in Terrific Broth medium at 37 °C until the OD₆₀₀ had reached 1.0–1.2. Expression was induced with addition of 0.5 mM isopropylthio- β -D-galactoside for 5 h at 20 °C. Cells were resuspended in chitin column equilibration buffer [20 mM Hepes (pH 7.5), 500 mM NaCl, 1 mM ethylenediaminetetraacetic acid, and 100 μ M PMSF]. After purification on the chitin affinity column and release of the protein by DTT-induced autocleavage of the intein, Spire_{366–482} was additionally purified on a reverse-phase C18 column (0.1% trifluoroacetic acid and 0–90% acetonitrile) and then dialyzed extensively against 25 mM Tris–HCl (pH 7.5) and 100 mM NaCl.

Crystallization of 3W-Actin and WxActin complexes

The complex of 3W-Actin (consisting of a tandem repeat of three W domains with three actin subunits bound²²) was dialyzed against 20 mM Hepes (pH 7.5), 100 mM NaCl, 0.2 mM CaCl₂, and 0.2 mM ATP, and concentrated

to 15 mg/ml using an Amicon centrifugal filter (Millipore). Needle-like crystals grow within hours or even minutes using the hanging-drop vapor diffusion method at 20 °C and from drops consisting of a 1:1 (vol/vol) mixture of protein solution and well solution containing 100 mM CAPS (pH 10.0) and 24% polyethylene glycol 3350. However, these crystals did not diffract the X-rays. Crystal quality and diffraction were improved with addition of 10–100 mM RbCl or polyvinylpyrrolidone K15 as additive. The crystals were flash frozen in liquid nitrogen, with addition of 20% glycerol as cryoprotectant. The cross-linked WxActin complex was concentrated to 5 mg/ml and crystallized using the hanging-drop vapor diffusion method at 20 °C from a well solution containing 0.2 M LiNO₃ and 20% polyethylene glycol 3350.

The content of the 3W-Actin crystals was analyzed by nonreducing gel electrophoresis and mass spectrometry, using a Voyager DE Pro MALDI-TOF Mass Spectrometer (Applied Biosystems) and sinapinic acid as matrix. For this analysis, multiple crystals were collected, washed five times through the crystallization solution by transferring them with a cryo loop, and then dissolved in water.

Data collection and determination of structures

X-ray data sets were collected from WxActin and 3W-Actin crystals at beamline 17-BM of the Industrial Macromolecular Crystallography Association Collaborative Access Team facility of the Advance Photon Source (Argonne, IL). Data indexing and scaling were carried out with the program HKL2000 (HKL Research, Inc.). The crystals of 3W-Actin diffracted only up to 7.0 Å resolution (Table 1). The data in the last resolution shell (7.25–7.0 Å) are weak ($I/\sigma = 1.1$) and only 34.3% complete. Yet, ~70% of the data were obtained between 7.9 Å and 7.0 Å, with an average I/σ of 2.1 and a redundancy of 6. This range includes 449 reflections (~20% of the total). Because of the limited resolution, special emphasis was placed on obtaining a highly redundant data set (the average redundancy is 20.5 for the entire data set), which should minimize intensity errors.

The structure of WxActin was determined by molecular replacement, using the structure of actin complexed with the W domain of WASP (PDB accession code 2A3Z) as search model. Molecular replacement and refinement were carried out with the program PHENIX,²⁹ and model building was performed with the program Coot.⁴⁷

The structure of 3W-Actin was determined by molecular replacement using the stronger data between 15 Å and 8 Å resolutions and independently with two different programs: Phaser³⁰ (belonging to the PHENIX package)²⁹ and AMoRe.³¹ The two programs gave the same solution. The likelihood-based scoring function of the program PHENIX is highly sensitive to the quality of the search model.⁴⁸ Several search models, including monomeric actin,³³ complexes of W-Actin determined as ternary complexes with DNase I,^{11,13} the complex of ciboulot-actin with bound latrunculin A,¹² the structure of actin with the C-terminal portion of Tβ4,⁴¹ and the structure of WxActin determined here, were tested. The best-contrasted solution was obtained using the structure of WxActin as search model. Two different models were prepared based on this structure: one consisting of the entire cross-linked complex and one lacking the cross-linked portion (i.e., the last five

amino acids of actin and the first three amino acids of the W domain). These two models were positioned independently using a multibody search and clearly defined the locations of the first (cross-linked) actin subunit and the second (non-cross-linked) actin subunit of the dimer.

While PHENIX was used in automated mode, a more exhaustive search was performed with the program AMoRe (details in Supplementary Material). AMoRe's self-rotation function gave a single prominent peak with a correlation coefficient of 0.62. Thus, while the volume of the unit cell seemed to be compatible with the presence of three W-Actin complexes in the asymmetric unit (corresponding to a Matthews coefficient V_m of 2.15 Å³/Da and a solvent content of 43%), only two were found (for a V_m of 3.23 Å³/Da and a solvent content of 62%). We tested many possible configurations in which the orientation of one W-Actin complex was constrained with respect to the other, according to the noncrystallographic 2-fold axis resulting from the self-rotation function. This gave a clearly contrasted solution for two W-Actin complexes where the correlation between the calculated structure factor amplitude and the observed structure factor amplitude was 0.66 (0.50 for the next peak that was not contrasted above background). Because of the limited resolution, the only refinement performed after molecular replacement was rigid-body refinement, using all the diffraction data available.

Actin polymerization assay

Pyrene-actin polymerization assays were carried out and analyzed as described previously,⁴⁹ using a Cary Eclipse fluorescence spectrophotometer (Varian). All experiments were performed at 20 °C. Prior to data acquisition, 2 μM Mg-ATP-actin (6% pyrene labeled) was mixed with different concentrations of construct 3W (25 nM, 250 nM, or 1 μM), Tβ4 (1 μM), and Spire (25 nM and 250 nM) in F-buffer [10 mM Tris-HCl (pH 7.5), 1 mM MgCl₂, 50 mM KCl, 1 mM ethylene glycol bis (*b*-aminoethyl ether) *N,N'*-tetraacetic acid, 0.02 mg/ml bovine serum albumin, 0.2 mM ATP, 1 mM DTT, and 0.1 mM Na₃N]. Note that the addition of DTT prevents the cross-linking of construct 3W to actin Cys374 during the polymerization assay. Polymerization rates were measured from the slope of the polymerization curve at 50% polymerization and converted into nanomolars per second, assuming that the total concentration of polymerizable actin monomers is 1.9 μM (2 – 0.1 μM, i.e., by subtracting the critical concentration for actin monomer addition to the barbed end from the total concentration of actin).⁴⁹ Steady-state experiments with varying Tβ4 or 3W concentrations were carried out under similar conditions by allowing actin to polymerize for 16 h.

The program DynDom³² was used to calculate the relative rotation of actin subunits in the crystal structures of longitudinal actin dimers. Illustrations of the structures were prepared with the program PyMOL (DeLano Scientific LLC).

PDB accession numbers

Coordinates and structure factors were deposited under PDB accession codes 3M1F (WxActin) and 3M3N (3W-Actin).

Supplementary materials related to this article can be found online at [doi:10.1016/j.jmb.2010.08.040](https://doi.org/10.1016/j.jmb.2010.08.040)

Acknowledgements

This work was supported by National Institutes of Health grant P01 HL086655. Use of beamline 17-BM at the Industrial Macromolecular Crystallography Association Collaborative Access Team facility was supported by the Industrial Macromolecular Crystallography Association through a contract with the Hauptman–Woodward Medical Research Institute. The Advanced Photon Source was supported by Department of Energy contract W-31-109-Eng-38.

References

- Sept, D. & McCammon, J. A. (2001). Thermodynamics and kinetics of actin filament nucleation. *Biophys. J.* **81**, 667–674.
- Pollard, T. D. & Borisy, G. G. (2003). Cellular motility driven by assembly and disassembly of actin filaments. *Cell*, **112**, 453–465.
- Holmes, K. C., Popp, D., Gebhard, W. & Kabsch, W. (1990). Atomic model of the actin filament. *Nature*, **347**, 44–49.
- Oda, T., Iwasa, M., Aihara, T., Maeda, Y. & Narita, A. (2009). The nature of the globular- to fibrous-actin transition. *Nature*, **457**, 441–445.
- Holmes, K. C. (2009). Structural biology: actin in a twist. *Nature*, **457**, 389–390.
- Dominguez, R. (2010). Structural insights into *de novo* actin polymerization. *Curr. Opin. Struct. Biol.* **20**, 217–225.
- Dominguez, R. (2009). Actin filament nucleation and elongation factors—structure–function relationships. *Crit. Rev. Biochem. Mol. Biol.* **44**, 351–366.
- Paunola, E., Mattila, P. K. & Lappalainen, P. (2002). WH2 domain: a small, versatile adapter for actin monomers. *FEBS Lett.* **513**, 92–97.
- Dominguez, R. (2007). The beta-thymosin/WH2 fold: multifunctionality and structure. *Ann. NY Acad. Sci.* **1112**, 86–94.
- Dominguez, R. (2004). Actin-binding proteins—a unifying hypothesis. *Trends Biochem. Sci.* **29**, 572–578.
- Chereau, D., Kerff, F., Graceffa, P., Grabarek, Z., Langsetmo, K. & Dominguez, R. (2005). Actin-bound structures of Wiskott–Aldrich syndrome protein (WASP)-homology domain 2 and the implications for filament assembly. *Proc. Natl Acad. Sci. USA*, **102**, 16644–16649.
- Hertzog, M., van Heijenoort, C., Didry, D., Gaudier, M., Coutant, J., Gigant, B. *et al.* (2004). The beta-thymosin/WH2 domain; structural basis for the switch from inhibition to promotion of actin assembly. *Cell*, **117**, 611–623.
- Lee, S. H., Kerff, F., Chereau, D., Ferron, F., Klug, A. & Dominguez, R. (2007). Structural basis for the actin-binding function of missing-in-metastasis. *Structure*, **15**, 145–155.
- Quinlan, M. E., Heuser, J. E., Kerkhoff, E. & Mullins, R. D. (2005). *Drosophila* Spire is an actin nucleation factor. *Nature*, **433**, 382–388.
- Ahuja, R., Pinyol, R., Reichenbach, N., Custer, L., Klingensmith, J., Kessels, M. M. & Qualmann, B. (2007). Cordon-bleu is an actin nucleation factor and controls neuronal morphology. *Cell*, **131**, 337–350.
- Liverman, A. D., Cheng, H. C., Trosky, J. E., Leung, D. W., Yarbrough, M. L., Burdette, D. L. *et al.* (2007). Arp2/3-independent assembly of actin by *Vibrio* type III effector VopL. *Proc. Natl Acad. Sci. USA*, **104**, 17117–17122.
- Tam, V. C., Serruto, D., Dziejman, M., Briehner, W. & Mekalanos, J. J. (2007). A type III secretion system in *Vibrio cholerae* translocates a formin/Spire hybrid-like actin nucleator to promote intestinal colonization. *Cell Host Microbe*, **1**, 95–107.
- Pollard, T. D. (2007). Regulation of actin filament assembly by Arp2/3 complex and formins. *Annu. Rev. Biophys. Biomol. Struct.* **36**, 451–477.
- Goley, E. D. & Welch, M. D. (2006). The ARP2/3 complex: an actin nucleator comes of age. *Nat. Rev. Mol. Cell Biol.* **7**, 713–726.
- Zuchero, J. B., Coutts, A. S., Quinlan, M. E., Thangue, N. B. & Mullins, R. D. (2009). p53-cofactor JMY is a multifunctional actin nucleation factor. *Nat. Cell Biol.* **11**, 451–459.
- Chereau, D., Boczkowska, M., Skwarek-Maruszewska, A., Fujiwara, I., Hayes, D. B., Rebowksi, G. *et al.* (2008). Leiomodrin is an actin filament nucleator in muscle cells. *Science*, **320**, 239–243.
- Rebowksi, G., Boczkowska, M., Hayes, D. B., Guo, L., Irving, T. C. & Dominguez, R. (2008). X-ray scattering study of actin polymerization nuclei assembled by tandem W domains. *Proc. Natl Acad. Sci. USA*, **105**, 10785–10790.
- Boczkowska, M., Rebowksi, G., Petoukhov, M. V., Hayes, D. B., Svergun, D. I. & Dominguez, R. (2008). X-ray scattering study of activated Arp2/3 complex with bound actin-WCA. *Structure*, **16**, 695–704.
- Schutt, C. E., Myslik, J. C., Rozycki, M. D., Gooneseckere, N. C. & Lindberg, U. (1993). The structure of crystalline profilin–beta-actin. *Nature*, **365**, 810–816.
- Ferron, F., Rebowksi, G., Lee, S. H. & Dominguez, R. (2007). Structural basis for the recruitment of profilin–actin complexes during filament elongation by Ena/VASP. *EMBO J.* **26**, 4597–4606.
- Baek, K., Liu, X., Ferron, F., Shu, S., Korn, E. D. & Dominguez, R. (2008). Modulation of actin structure and function by phosphorylation of Tyr-53 and profilin binding. *Proc. Natl Acad. Sci. USA*, **105**, 11748–11753.
- Aguda, A. H., Burtnick, L. D. & Robinson, R. C. (2005). The state of the filament. *EMBO Rep.* **6**, 220–226.
- Renault, L., Bugyi, B. & Carlier, M. F. (2008). Spire and Cordon-bleu: multifunctional regulators of actin dynamics. *Trends Cell. Biol.* **18**, 494–504.
- Zwart, P. H., Afonine, P. V., Grosse-Kunstleve, R. W., Hung, L. W., Ioerger, T. R., McCoy, A. J. *et al.* (2008). Automated structure solution with the PHENIX suite. *Methods Mol. Biol.* **426**, 419–435.
- McCoy, A. J., Grosse-Kunstleve, R. W., Adams, P. D., Winn, M. D., Storoni, L. C. & Read, R. J. (2007). Phaser crystallographic software. *J. Appl. Crystallogr.* **40**, 658–674.

31. Navaza, J. (2001). Implementation of molecular replacement in AMoRe. *Acta Crystallogr. Sect. D*, **57**, 1367–1372.
32. Hayward, S. & Berendsen, H. J. (1998). Systematic analysis of domain motions in proteins from conformational change: new results on citrate synthase and T4 lysozyme. *Proteins*, **30**, 144–154.
33. Rould, M. A., Wan, Q., Joel, P. B., Lowey, S. & Trybus, K. M. (2006). Crystal structures of expressed non-polymerizable monomeric actin in the ADP and ATP states. *J. Biol. Chem.* **281**, 31909–31919.
34. Allingham, J. S., Zampella, A., D'Auria, M. V. & Rayment, I. (2005). Structures of microfilament destabilizing toxins bound to actin provide insight into toxin design and activity. *Proc. Natl Acad. Sci. USA*, **102**, 14527–14532.
35. Rizvi, S. A., Tereshko, V., Kossiakoff, A. A. & Kozmin, S. A. (2006). Structure of bistramide A-actin complex at a 1.35 Å resolution. *J. Am. Chem. Soc.* **128**, 3882–3883.
36. Kudryashov, D. S., Sawaya, M. R., Adisetiyo, H., Norcross, T., Hegyi, G., Reisler, E. & Yeates, T. O. (2005). The crystal structure of a cross-linked actin dimer suggests a detailed molecular interface in F-actin. *Proc. Natl Acad. Sci. USA*, **102**, 13105–13110.
37. Sawaya, M. R., Kudryashov, D. S., Pashkov, I., Adisetiyo, H., Reisler, E. & Yeates, T. O. (2008). Multiple crystal structures of actin dimers and their implications for interactions in the actin filament. *Acta Crystallogr. Sect. D*, **64**, 454–465.
38. Otomo, T., Tomchick, D. R., Otomo, C., Panchal, S. C., Machius, M. & Rosen, M. K. (2005). Structural basis of actin filament nucleation and processive capping by a formin homology 2 domain. *Nature*, **433**, 488–494.
39. Klenchin, V. A., Khaitlina, S. Y. & Rayment, I. (2006). Crystal structure of polymerization-competent actin. *J. Mol. Biol.* **362**, 140–150.
40. Reisler, E. & Egelman, E. H. (2007). Actin structure and function: what we still do not understand. *J. Biol. Chem.* **282**, 36133–36137.
41. Irobi, E., Aguda, A. H., Larsson, M., Guerin, C., Yin, H. L., Burtnick, L. D. *et al.* (2004). Structural basis of actin sequestration by thymosin-beta4: implications for WH2 proteins. *EMBO J.* **23**, 3599–3608.
42. Weber, A., Nachmias, V. T., Pennise, C. R., Pring, M. & Safer, D. (1992). Interaction of thymosin beta 4 with muscle and platelet actin: implications for actin sequestration in resting platelets. *Biochemistry*, **31**, 6179–6185.
43. Xue, B., Aguda, A. H. & Robinson, R. C. (2007). Models of the actin-bound forms of the beta-thymosins. *Ann. NY Acad. Sci.* **1112**, 56–66.
44. Hertzog, M., Yarmola, E. G., Didry, D., Bubb, M. R. & Carlier, M. F. (2002). Control of actin dynamics by proteins made of beta-thymosin repeats: the actobindin family. *J. Biol. Chem.* **277**, 14786–14792.
45. Van Troys, M., Ono, K., Dewitte, D., Jonckheere, V., De Ruyck, N., Vandekerckhove, J. *et al.* (2004). Tetrathymosinbeta is required for actin dynamics in *Caenorhabditis elegans* and acts via functionally different actin-binding repeats. *Mol. Biol. Cell*, **15**, 4735–4748.
46. Pardee, J. D. & Spudich, J. A. (1982). Purification of muscle actin. *Methods Enzymol.* **85**, 164–181.
47. Emsley, P. & Cowtan, K. (2004). Coot: model-building tools for molecular graphics. *Acta Crystallogr. Sect. D*, **60**, 2126–2132.
48. McCoy, A. J., Grosse-Kunstleve, R. W., Storoni, L. C. & Read, R. J. (2005). Likelihood-enhanced fast translation functions. *Acta Crystallogr. Sect. D*, **61**, 458–464.
49. Harris, E. S. & Higgs, H. N. (2006). Biochemical analysis of mammalian formin effects on actin dynamics. *Methods Enzymol.* **406**, 190–214.